


Article

Chaotic Itinerancy in Random Dynamical System Related to Associative Memory Models

Ricardo Bioni Liberalquino ¹, Maurizio Monge ¹, Stefano Galatolo ^{2,*}  and Luigi Marangio ³

¹ Institute of Mathematics, Universidade Federal do Rio de Janeiro, 21941-901 Rio de Janeiro, Brazil; ricardo.bioni@hotmail.com (R.B.L.); maurizio.monge@im.ufrj.br (M.M.)

² Dipartimento di Matematica, Università di Pisa, 56126 Pisa, Italy

³ Femto-ST Institute, Université de Bourgogne Franche-Comté, 21000 Dijon, France; lmarangio@gmail.com

* Correspondence: galatolo@dm.unipi.it

Received: 31 January 2018; Accepted: 28 February 2018; Published: 7 March 2018

Abstract: We consider a random dynamical system arising as a model of the behavior of a macrovariable related to a more complicated model of associative memory. This system can be seen as a small (stochastic and deterministic) perturbation of a deterministic system having two weak attractors which are destroyed after the perturbation. We show, with a computer aided proof, that the system has a kind of chaotic itinerancy. Typical orbits are globally chaotic, while they spend a relatively long time visiting the attractor's ruins.

Keywords: chaotic itinerancy; computer aided proof; neural networks

1. Introduction

Chaotic itinerancy is a concept used to refer to a dynamical behavior in which typical orbits visit a sequence of regions of the phase space called “quasi attractors” or “attractor ruins” in some irregular way. Informally speaking, during this itinerancy, the orbits visit a neighborhood of a quasi attractor (the attractor ruin) with a relatively regular and stable motion, for relatively long times and then the trajectory jumps to another quasi attractor of the system after a relatively small chaotic transient. This behavior was observed in several models and experiments related to the dynamics of neural networks and related to neurosciences (see [1]). In this itinerancy, the visit near some attractors was associated to the appearance of some macroscopic aspect of the system, like the emergence of a perception or a memory, while the chaotic iterations from a quasi attractor to another are associated to an intelligent (history dependent with trial and errors) search for the next thought or perception (see [2]). This kind of phenomena was observed in models of the neural behavior which are fast-slow systems or random dynamical systems (sometimes modeling as a random system the fast-slow behavior).

As far as we know the concept did not have a complete mathematical formalization though in [3] some mathematical scenarios are presented, showing some situations in which these phenomena may appear. Often this phenomenon is associated to the presence of some kind of “weak” attractor, as Milnor type attractors (see e.g., [3] or [4]) in the system and to small perturbations allowing typical trajectories to escape the attractor. Chaotic itinerancy was found in many applied contexts, but a systematic treatment of the literature is out of the scope of this paper, for which we invite the reader to consult [1] for a wider introduction to the subject and to its literature.

In this paper, our goal is to investigate and illustrate this concept from a mathematical point of view with some meaningful examples. We consider a simple one-dimensional random map derived from the literature on the subject (see Section 3). This map is a relatively simple discrete time random dynamical system on the interval, suggested by the behavior of certain macrovariables in the neural networks studied in [5], modeling the neocortex with a variant of Hopfield's asynchronous recurrent neural

network presented in [6]. In Hopfield’s network, memories are represented by stable attractors and an unlearning mechanism is suggested in [7] to account for unpinning of these states (see also, e.g., [8]). In the network presented in [5], however, these are replaced by Milnor attractors, which appear due to a combination of symmetrical and asymmetrical couplings and some resetting mechanism. A similar map is also obtained in [9], in the context of the BvP neuron driven by a sinusoidal external stimulus. They belong to a family known as Arnold circle maps (named after [10]), which are useful in physiology (see [11] (Equation (3))). The simple model we study shares with the more complicated models from which it is derived the presence of quasi attractors (it can be seen as a stochastic perturbation of a system with Milnor attractors), its understanding can bring some light on the mathematical understanding of chaotic itineracy.

The model we consider is made by a deterministic map T on the circle perturbed by a small additive noise. For a large enough noise, its associated random dynamical system exhibits an everywhere positive stationary density concentrated on a small region (see [12] for an analytical treatment), which can be attributed to the chaotic itinerancy of the neural network.

In the paper, with the help of a computer aided proof, we establish several results about the statistical and geometrical properties of the above system, with the goal to show that “the behavior of this system exhibits a kind of chaotic itineracy”. We show that the system is (exponentially) mixing, hence globally chaotic. We also show a rigorous estimate of the density of probability (and then the frequency) of visits of typical trajectories near the attractors, showing that this is relatively high with respect to the density of probability of visits in other parts of the space. This is done by a computer aided rigorous estimate of the stationary probability density of the system. The computer aided proof is based on the approximation of the transfer operator of the real system by a finite rank operator which is rigorously computed and whose properties are estimated by the computer. The approximation error from the real system to the finite rank one is then managed using an appropriated functional analytic approach developed in [13] for random systems (see also [14–16] for applications to deterministic dynamics or iterated functions systems).

The paper is structured as follows. In Section 2, we review basic definitions related to random dynamical systems, in particular, the Perron-Frobenius operator, which will play a major role. In Section 3, we present our example along with an explanation of the method used to study it. The numerical results supported by the previous theoretical sections are presented in Section 4, while in Section 5 we present a conclusion with some additional comments.

2. Random Dynamical Systems

This section follows [17,18]. We denote by (X, \mathcal{X}, p) a probability space and by (M, \mathcal{A}, μ) the corresponding space of sequences (over \mathbb{N} or \mathbb{Z}), with the product σ -algebra and probability measure. In addition, we denote by f the shift map on M , $f(\{x_i\}_{i \in I}) = \{x_{i+1}\}_{i \in I}$, where $I = \mathbb{N}_0$ or \mathbb{Z} .

Definition 1. Let (N, \mathcal{B}) be a measurable space. Endow $M \times N$ with the product σ -algebra $\mathcal{A} \otimes \mathcal{B}$. A random transformation over f is a measurable transformation of the form

$$F : M \times N \rightarrow M \times N, \quad F(x, y) = (f(x), F_x(y)),$$

where $x \mapsto F_x$ depends only on the zeroth coordinate of x .

Suppose we have a (bounded, measurable) function $\phi : N \rightarrow \mathbb{R}$. Given a random orbit $\{y_i\}_{i \in I}$, for which we know the value of $y_0 = v \in N$, we may ask what is the expected value for $\phi(y_1)$, that is, $\mathbb{E}(\phi(y_1)|y_0 = v)$. Since the iterate depends on an outcome $x \in M$, which is distributed according to μ , this can be calculated as

$$U\phi(v) = \int_M \phi(F_x(v)) d\mu(x).$$

The equation above defines the *transition operator* associated with the random transformation F as an operator in the space $L^\infty(m)$ of bounded measurable functions. Dually, we can consider its *adjoint transition operator* (These operators are related by $\int \phi d(U^*\eta) = \int (U\phi) d\eta$, for every bounded measurable $\phi : N \rightarrow \mathbb{R}$ (see [18] (lemma 5.3)).) that acts in the space of probability measures η on N , defined by

$$U^*\eta(B) = \int (F_x)_*\eta(B) d\mu(x) = \int \eta(F_x^{-1}(B)) d\mu(x).$$

Of particular importance are the fixed points of the operator U^* .

Definition 2. A probability measure η for N is called *stationary for the random transformation F* if $U^*\eta = \eta$.

We recall the deterministic concept of invariant measures.

Definition 3. If $h : C \rightarrow C$ is a measurable mapping in the measurable space (C, \mathcal{C}) , we say ν is an *invariant measure for h* if $\nu(h^{-1}(E)) = \nu(E)$ for any measurable $E \subset C$.

In the one-sided case ($M = X^{\mathbb{N}}$), invariant measures and stationary measures for F are related by the following proposition.

Proposition 1 ([18] (proposition 5.4)). A probability measure η on N is stationary for F if and only if $\mu \times \eta$ is invariant for F .

Another concept from deterministic dynamical systems that can be naturally extended to random dynamical systems is that of ergodicity.

Definition 4. Suppose η is stationary for F . We say that η is *ergodic for F* if either

1. every (bounded measurable) function ϕ that is η -stationary, i.e., $U\phi = \phi$, is constant in some full η -measure set;
2. every set B that is η -stationary, i.e., whose characteristic function χ_B is η -stationary, has full or null η -measure.

In fact, both conditions are equivalent (see [18] (proposition 5.10)). In the one-sided case, the following proposition relates ergodicity of a random dynamical system with the deterministic concept.

Proposition 2. A stationary measure η is ergodic for F if and only if $\mu \times \eta$ is an ergodic F -invariant measure.

Suppose N is a manifolds with boundary and consider its Lebesgue measure m . It's useful to consider the measures which are absolutely continuous and the effect of U^* upon their densities. This is possible, for example, if $(F_x)_*m$ is absolutely continuous for every $x \in X$.

Definition 5. The *Perron-Frobenius operator with respect to the random transformation F* is the operator (This is an extension to the deterministic case, in which the Koopman operator $Uf = f \circ F$ is used instead of the transition operator.)

$$L : L^1(m) \rightarrow L^1(m), \quad Lf = \frac{dU^*(fm)}{dm}.$$

We can use the Perron-Frobenius operator to define a mixing property.

Proposition 3. We say that a stationary measure $\eta = h dm$ is *mixing for F* if the Perron-Frobenius operator L satisfies

$$\lim_{n \rightarrow \infty} \int L^n(f)g dm = \int f dm \int gh dm$$

for every $f \in L^1(m)$ and $g \in L^\infty(m)$ (This definition is adapted from [19] (Equation (1.5)).).

Since L and U are dual, the mixing condition can be restated as

$$\lim_{n \rightarrow \infty} \int U^n(g)f \, d\eta = \int g \, d\eta \int f \, d\eta$$

for every $f \in L^1(\eta)$ and $g \in L^\infty(\eta)$, which is similar to the usual definition of decay of correlations.

If F is mixing, then F is ergodic for η (see [17] (Theorem 4.4.1)). In our example, we shall verify the following stronger condition.

$$\|L^n|_V\|_{L^1(m) \rightarrow L^1(m)} \rightarrow 0, \quad V = \left\{ f \in L^1(m) : \int f \, dm = 0 \right\}. \tag{1}$$

Remark 1. It suffices to verify that $\|L^n|_V\|_{L^1(m) \rightarrow L^1(m)} < 1$ for some $n \in \mathbb{N}$, because $\|L_\xi\|_{L^1} = 1$.

Proposition 4. If the Perron-Frobenius operator L of a random dynamical system F satisfies Equation (1), then L admits a unique stationary density h and F is mixing.

Proof. $\|L\|_{L^1(m)} = 1$ because L is a Markov operator [17] (Remark 3.2.2). Take a density $f \in L^1(m)$. We claim that $L^n(f) \rightarrow h$ for some density h . On the contrary, there would be $\epsilon > 0$ and a subsequence $\{L^{n_k}(f)\}_{k \in \mathbb{N}}$ such that

$$\forall k \in \mathbb{N} : \|L^{n_{k+1}}(f) - L^{n_k}(f)\|_{L^1(m)} \geq \epsilon.$$

$L^{n_{k+1}-n_k}(f) - f \in V$ because $L^{n_{k+1}-n_k}(f)$ is a density, and $2\|L|_V\|_{L^1(m)}^{n_k} \geq \epsilon$ for every $k \in \mathbb{N}$, a contradiction.

h is stationary because L is bounded, and unique because $g - h \in V$ implies $\|L^n(g) - h\|_{L^1(m)} \rightarrow 0$ for any density g . Similarly, the mixing property follows from $f - (\int f \, dm)h \in V$. \square

Remark 2. Any density f must converge exponentially fast to the stationary density h . Precisely, given N and $\alpha < 1$ such that $\|L^N\|_{L^1(m)} \leq \alpha$, the fact that $f - h \in V$ implies that $\|L^n(f) - h\|_{L^1(m)} \leq C\lambda^n$ for some $C > 0$ and $\lambda = \alpha^{1/N} < 1$.

In the following, we will use Equation (1) as the definition of mixing property.

3. A Neuroscientifically Motivated Example

In [5], a neural network showing successive memory recall without instruction, inspired by Hopfield’s asynchronous neural network and the structure of the mammalian neocortex, is presented.

A macrovariable, related to the “activity” of the network (see Figure 1, similar plots appeared also in [5,20]) was observed to evolve as a noisy one dimensional map in the case that the network receives no external stimulus (its definition of can be found in [5] (p. 6)). This was regarded in [20] as related to a rule of successive association of memory, exhibiting chaotic dynamics.

This behavior can be modeled as a random dynamical system T_ξ , with a deterministic component given by an Arnold circle map (see Figure 2) and a stochastic part given by a random additive noise. The system can be hence defined as

$$x_{n+1} = T(x_n) + \xi_n \pmod{1}, \text{ where } T(v) = v + A \sin(4\pi v) + C, \tag{2}$$

for $A = 0.08$, $C = 0.1$ and ξ_n an i.i.d. sequence of random variables with a distribution assumed uniform over $[-\xi, \xi]$.

The Perron-Frobenius operator (Definition 5) associated to this system is given by $L_\xi = N_\xi L$ (a proof can be found in [17] (p. 327)), where N_ξ is a convolution operator (Equation (3)) and L is the Perron-Frobenius operator of T .

$$N_\xi f(t) = \xi^{-1} \int_{-\xi/2}^{\xi/2} f(t - \tau) d\tau. \tag{3}$$

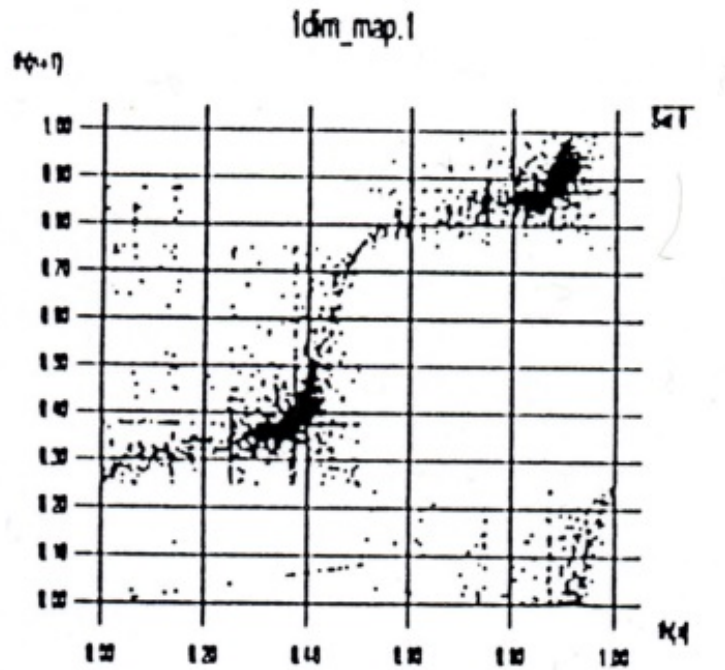


Figure 1. Data plot suggesting the model we studied ([21]).

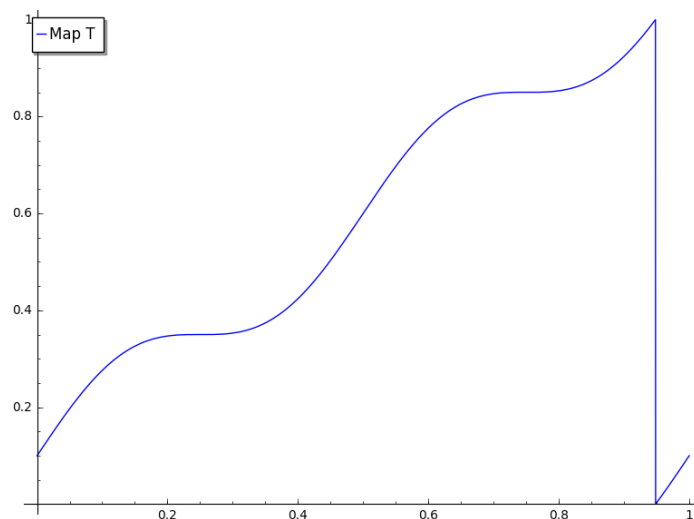


Figure 2. Deterministic component of Equation (2).

It is well known that such an operator has an invariant probability density in L^1 . In the following, we show that L_ξ can be rigorously approximated and a mixing property can be proved using the numerical estimates.

In addition, a rigorous approximation of the stationary density of L_{ξ} is obtained, from which we can conclude the existence of a kind of chaotic itinerancy.

Rigorous Approximation

Here we show how we can study the behavior of the Perron-Frobenius operator associated to Equation (2) by approximating it by a finite rank operator. The finite rank approximation we use is known in literature as Ulam’s method. For more details, see [13].

Suppose we are given a partition of \mathbb{S}^1 into intervals $\mathcal{I}_{\delta} = \{I_i\}_{i=1}^n$ and denote the characteristic function of I_i by χ_i . An operator $L : L^1(\mathbb{S}^1) \rightarrow L^1(\mathbb{S}^1)$ can be discretized by

$$L_{\delta} : L^1(\mathbb{S}^1) \rightarrow L^1(\mathbb{S}^1), \quad L_{\delta} = \pi_{\delta} L \pi_{\delta},$$

where $\pi_{\delta} : L^1(\mathbb{S}^1) \rightarrow L^1(\mathbb{S}^1)$ is the projection

$$\pi_{\delta} h(x) = \sum_{i=1}^n \mathbb{E}(h|I_i) \chi_i.$$

This operator is completely determined by its restriction to the subspace generated by $\{\chi_1, \dots, \chi_n\}$, and thus may be represented by a matrix in this base, which we call the Ulam matrix. In the following, we assume that $\delta > 0$ and \mathcal{I}_{δ} is a partition of $[0, 1] \pmod{1} \cong \mathbb{S}^1$ with diameter $< \delta$.

For computational purposes, the operator L_{ξ} is discretized as

$$L_{\delta, \xi} = \pi_{\delta} N_{\xi} \pi_{\delta} L \pi_{\delta}.$$

This is simple to work with because it is the product of the discretized operators $\pi_{\delta} N_{\xi} \pi_{\delta}$ and $\pi_{\delta} L \pi_{\delta}$.

Let $V = \{f \in L^1(m) : \int f dm = 0\}$ and denote by f_{ξ} and $f_{\xi, \delta}$ the stationary probability densities for L_{ξ} and $L_{\delta, \xi}$, respectively. Suppose $\|L_{\delta, \xi}^n\| \leq \alpha < 1$ for some $n \in \mathbb{N}$. Since

$$\|L_{\xi}^i|_V\|_{L^1} \leq \|L_{\delta, \xi}^i|_V\|_{L^1} + \|L_{\delta, \xi}^i|_V - L_{\xi}^i|_V\|_{L^1} \tag{4}$$

and ([13] (Equation (2)))

$$\|f_{\xi} - f_{\xi, \delta}\|_{L^1} \leq \frac{1}{1 - \alpha} \|(L_{\delta, \xi}^n - L_{\xi}^n)f_{\xi}\|_{L^1}, \tag{5}$$

we search a good estimate of $\|(L_{\delta, \xi}^n - L_{\xi}^n)f_{\xi}\|_{L^1}$ to prove both mixing of T_{ξ} and give a rigorous estimate of $\|f_{\xi} - f_{\xi, \delta}\|_{L^1}$.

Since the calculus of $\|L_{\delta, \xi}^i|_V\|$ is computationally complex, an alternative approach is used in [13] (see [22] for a previous application of a similar idea to deterministic dynamics). First, we use a coarser version of the operator, $L_{\delta_{\text{contr}}, \xi}$, where δ_{contr} is a multiple of δ . Then, we determine $n_{\text{contr}} \in \mathbb{N}$ and constants $C_{i, \text{contr}}$, for $i < n_{\text{contr}}$, and $\alpha_{\text{contr}} < 1$ in order that

$$\|L_{\delta_{\text{contr}}, \xi}^i\| \leq C_{i, \text{contr}}, \quad \|L_{\delta_{\text{contr}}, \xi}^{n_{\text{contr}}}|_V\| \leq \alpha_{\text{contr}}. \tag{6}$$

Finally, the following lemma from [13] is used.

Lemma 1. *Let $\|L_{\gamma, \xi}^i|_V\|_{L^1} \leq C_i(\gamma)$; let σ be a linear operator such that $\sigma^2 = \sigma$, $\|\sigma\|_{L^1} \leq 1$, and $\sigma \pi_{\gamma} = \pi_{\gamma} \sigma = \pi_{\gamma}$; let $\Lambda = \sigma N_{\xi} \sigma L$. Then we have*

$$\|(L_{\gamma, \xi}^n - \Lambda^n)N_{\xi}\|_{L^1} \leq \frac{\gamma}{\xi} \cdot \left(2 \sum_{i=0}^{n-1} C_i(\gamma) + 1\right) \tag{7}$$

It is applied to two cases.

1. $\gamma = \delta_{\text{contr}}, \sigma = \pi_\delta$ and $\Lambda = L_{\delta, \bar{\zeta}}$ implies

$$\|(L_{\delta_{\text{contr}}, \bar{\zeta}}^n - L_{\delta, \bar{\zeta}}^n)N_{\bar{\zeta}}\|_{L^1} \leq \frac{\delta}{\bar{\zeta}} \cdot \left(2 \sum_{i=0}^{n-1} C_{i, \text{contr}} + 1\right).$$

This is used to obtain $n \in \mathbb{N}, \alpha < 1$ and $C_i, i < n$, such that

$$\|L_{\delta, \bar{\zeta}}^i|_V\| \leq C_i, \|L_{\delta, \bar{\zeta}}^n|_V\| \leq \alpha. \tag{8}$$

2. $\gamma = \delta, \sigma = \text{Id}$ and $\Lambda = L_{\bar{\zeta}}$ implies

$$\begin{aligned} \|L_{\bar{\zeta}}^{n+1}|_V\|_{L^1} &\leq \|L_{\delta, \bar{\zeta}}^n L_{\bar{\zeta}}|_V\|_{L^1} + \|(L_{\bar{\zeta}}^n - L_{\delta, \bar{\zeta}}^n)L_{\bar{\zeta}}\|_{L^1} \\ &\leq \alpha + \frac{\delta}{\bar{\zeta}} \left(2 \sum_{i=0}^{n-1} C_i(\delta) + 1\right). \end{aligned}$$

By Remark 1, we conclude that the mixing condition is satisfied whenever

$$\lambda = \alpha + \frac{\delta}{\bar{\zeta}} \left(2 \sum_{i=0}^{n-1} C_i(\delta) + 1\right) < 1.$$

We remark that a simple estimate to Equation (5) is given by ([13] (Equation (4)))

$$\|f_{\bar{\zeta}} - f_{\bar{\zeta}, \delta}\|_{L^1} \leq \frac{1 + 2 \sum_{i=0}^{n-1} C_i}{2(1 - \alpha)} \delta \bar{\zeta}^{-1} \text{Var}(\rho). \tag{9}$$

The analysis of data obtained from the numerical approximation \tilde{f} of $f_{\delta, \bar{\zeta}}$, in particular its variance, allows the algorithm in [13] to improve greatly this bound, using interval arithmetic. In Table 1, the value `l1apriori` obtained from the first estimate Equation (9) and the best estimate `l1err` are compared.

4. Results

We verified mixing and calculated the stationary density for the one dimensional system Equation (2) using the numerical tools from the `compinv-meas` project (see [13]), which implements the ideas presented in Section 3. The data obtained is summarized in Table 1.

Table 1. Summary of the L^1 bounds on the approximation error obtained for the range of noises $\bar{\zeta}$, where n_{contr} and α_{contr} are chosen in order to satisfy Equation (6) so that the values α and $\sum C_i$ obtained through Lemma 1 attempt to minimize the error `l1err` obtained through the algorithm in [13].

$\bar{\zeta}$	n_{contr}	α_{contr}	α	$\sum C_i$	<code>l1apriori</code>	<code>l1err</code>
0.732×10^{-1}	126	0.027	0.05	56.64	0.313×10^{-2}	0.715×10^{-4}
0.610×10^{-1}	167	0.034	0.067	78.66	0.530×10^{-2}	0.105×10^{-3}
0.488×10^{-1}	231	0.051	0.1	120.56	0.106×10^{-1}	0.184×10^{-3}
0.427×10^{-1}	278	0.068	0.14	156.45	0.163×10^{-1}	0.268×10^{-3}
0.366×10^{-1}	350	0.087	0.19	213.17	0.273×10^{-1}	0.432×10^{-3}
0.305×10^{-1}	453	0.12	0.26	307.03	0.523×10^{-1}	0.813×10^{-3}
0.275×10^{-1}	532	0.14	0.32	380.64	0.776×10^{-1}	0.122×10^{-2}
0.244×10^{-1}	596	0.19	0.41	467.70	0.124	0.202×10^{-2}

Here $\delta = 2^{-19}$ is used to calculate the invariant density. $\delta_{\text{contr}} = 2^{-14}$: Used to find the estimates in Equation (6). $\delta_{\text{est}} = 2^{-12}$: Used to estimate the L^1 error of the invariant density

For an explanation of the values calculated, refer to Section 3. In the column `l1apriori`, we have the estimate Equation (9) for the approximation error of the stationary density in L^1 and in `l1err`, the improved estimate as in [13] (Section 3.2.5).

In every case, we used the following sizes of the partition.

In Figure 3, stationary densities obtained with this method are shown.

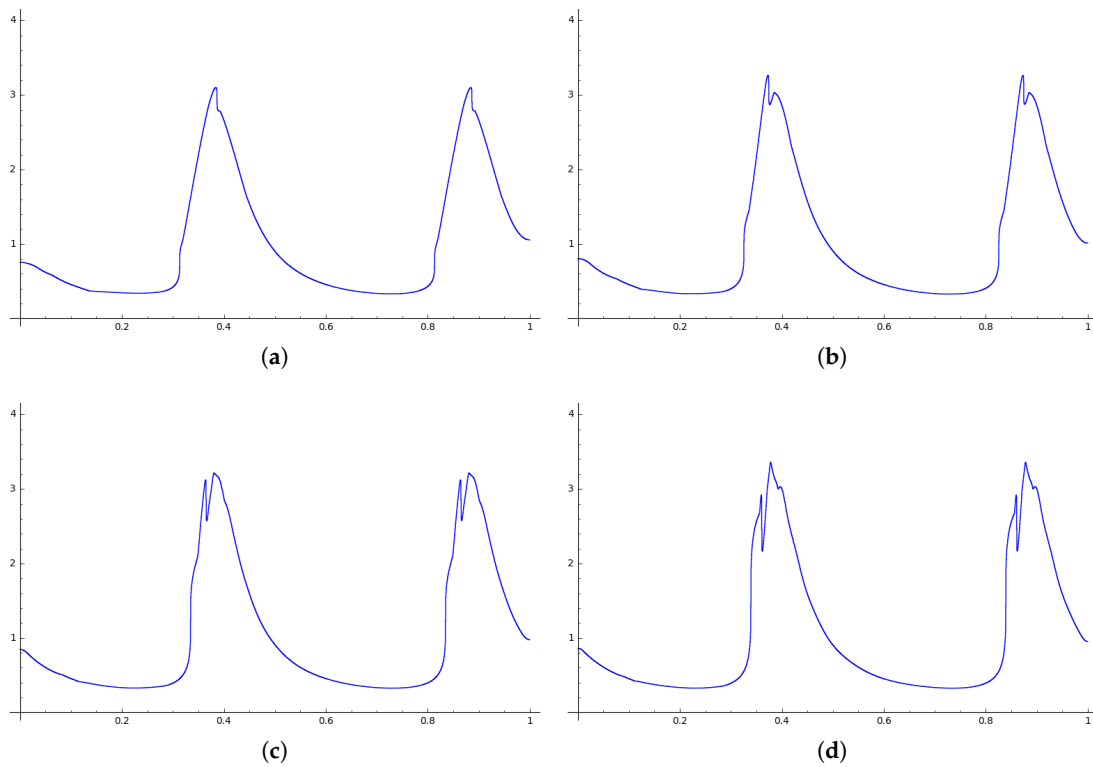


Figure 3. Approximated stationary densities $f_{\xi, \delta}$ for T_{ξ} , with $\delta = 2^{-19}$ and $A = 0.08$. (a) $\xi = 0.732 \times 10^{-1}$; (b) $\xi = 0.488 \times 10^{-1}$; (c) $\xi = 0.305 \times 10^{-1}$; (d) $\xi = 0.214 \times 10^{-1}$.

We also studied the system Equation (2) in the case that $A = 0.07$ for the same range of noises (Table 2). In Figure 4, stationary densities obtained in this case are shown. We note that the same kind of “chaotic itinerancy” obtained in the main case is observed.

Table 2. Summary of the L^1 bounds on the approximation error obtained for the range of noises ξ , for the system Equation (2) with the alternative value $A = 0.07$.

ξ	n_{contr}	α_{contr}	α	$\sum C_i$	<code>l1apriori</code>	<code>l1err</code>
0.732×10^{-1}	183	0.03	0.059	83.57	0.466×10^{-2}	0.255×10^{-4}
0.610×10^{-1}	237	0.046	0.089	119.31	0.822×10^{-2}	0.282×10^{-4}
0.488×10^{-1}	332	0.069	0.14	186.80	0.170×10^{-1}	0.323×10^{-4}
0.427×10^{-1}	406	0.087	0.18	244.95	0.267×10^{-1}	0.358×10^{-4}
0.366×10^{-1}	494	0.12	0.25	330.89	0.459×10^{-1}	0.419×10^{-4}
0.305×10^{-1}	500	0.3	0.46	419.92	0.974×10^{-1}	0.646×10^{-4}
0.275×10^{-1}	596	0.32	0.52	517.97	0.151	0.807×10^{-4}
0.244×10^{-1}	600	0.49	0.73	573.04	0.326	0.189×10^{-3}

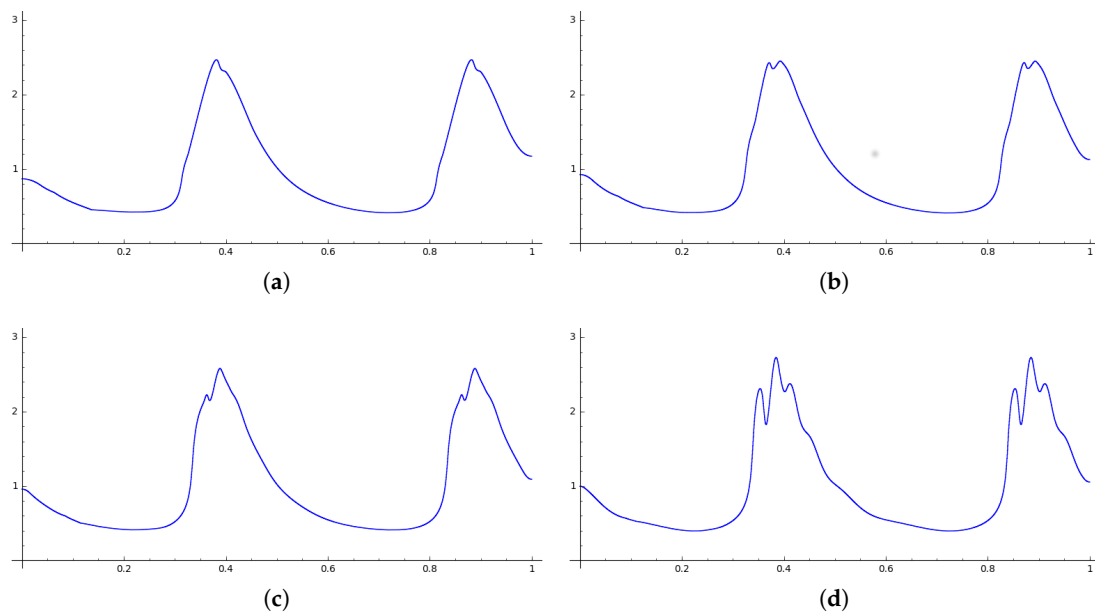


Figure 4. Approximated stationary densities $f_{\xi, \delta}$ for T_{ξ} , with $\delta = 2^{-19}$ and $A = 0.07$. (a) $\xi = 0.732 \times 10^{-1}$; (b) $\xi = 0.488 \times 10^{-1}$; (c) $\xi = 0.305 \times 10^{-1}$; (d) $\xi = 0.214 \times 10^{-1}$.

5. Conclusions

We have shown how the numerical approach developed in [13] can be used to study dynamical properties for a one dimensional random dynamical system of interest in the areas of physiology and neural networks.

In particular, we established mixing of the system and a rigorous estimate of its stationary density, which allowed us to observe that the trajectories concentrate in certain “weakly attracting” and “low chaotic” regions of the space, in concordance with the concept of chaotic itinerancy. The concept itself still did not have a complete mathematical formalization, and deeper understanding of the systems where it was found is important to extract its characterizing mathematical aspects.

The work we have done is only preliminary, to obtain some initial rigorous evidence of the chaotic itinerancy in the system. Further investigations are important to understand the phenomenon more deeply. Firstly, it would be important to understand more precisely the nature of the phenomenon: rigorously computing Lyapunov exponents and other chaos indicators. It would also be important to investigate the robustness of the behavior of the system under various kinds of perturbations, including the zero noise limit. Another important direction is to refine the model to adapt it better to the experimental data shown in Figure 1, with a noise intensity which depends on the point.

Author Contributions: All authors contributed to this article equally.

Conflicts of Interest: The authors declare no conflicts of interest.

References

1. Ichiro Tsuda (2013) Chaotic Itinerancy. Scholarpedia, 8(1):4459. Available online: http://www.scholarpedia.org/article/Chaotic_itinerancy (accessed on 27 February 2018).
2. Tsuda, I. Chaotic itinerancy and its roles in cognitive neurodynamics. *Curr. Opin. Neurobiol.* **2015**, *31*, 67–71.
3. Tsuda, I. Hypotheses on the functional roles of chaotic transitory dynamics. *Chaos* **2009**, *19*, 015113.
4. John, W. Milnor (2006) Attractor. Scholarpedia, 1(11):1815. Available online: <http://www.scholarpedia.org/article/Attractor> (accessed on 27 February 2018).
5. Tsuda, I.; Koerner, E.; Shimizu, H. Memory dynamics in asynchronous neural networks. *Prog. Theor. Phys.* **1987**, *78*, 51–71.

6. Hopfield, J.J. Neural networks and physical systems with emergent collective computational abilities. *Proc. Natl. Acad. Sci. USA* **1982**, *79*, 2554–2558.
7. Hopfield, J.J.; Feinstein, D.I.; Palmer, R.G. ‘Unlearning’ has a stabilizing effect in collective memories. *Nature* **1983**, *304*, 158–159.
8. Hoshino, O.; Usuba, N.; Kashimori, Y.; Kambara, T. Role of itinerancy among attractors as dynamical map in distributed coding scheme. *Neural Netw.* **1997**, *10*, 1375–1390.
9. Zeller, M.; Bauer, M.; Martienssen, W. Neural dynamics modeled by one-dimensional circle maps. *Chaos Solitons Fractals* **1995**, *5*, 885–893.
10. Arnold, V.I. Small denominators. I. Mappings of the circumference onto itself. *Am. Math. Soc. Transl. Ser. 2* **1965**, *46*, 213–284.
11. Glass, L. Synchronization and rhythmic processes in physiology. *Nature* **2001**, *410*, 277–284.
12. Zmarrou, H.; Humburg, A.J. Dynamics and bifurcations of random circle diffeomorphism. *Discrete Contin. Dyn. Syst. B* **2008**, *10*, 719–731.
13. Galatolo, S.; Monge, M.; Nisoli, I. Existence of Noise Induced Order, a Computer Aided Proof. Available online: <http://arxiv.org/pdf/1702.07024v2.pdf> (accessed on 27 February 2018).
14. Galatolo, S.; Nisoli, I. An elementary approach to rigorous approximation of invariant measures. *SIAM J. Appl. Dyn. Syst.* **2014**, *13*, 958–985.
15. Galatolo, S.; Nisoli, I. Rigorous computation of invariant measures and fractal dimension for maps with contracting fibers: 2D Lorenz-like maps. *Ergod. Theory Dyn. Syst.* **2016**, *36*, 1865–1891.
16. Galatolo, S.; Monge, M.; Nisoli, I. Rigorous approximation of stationary measures and convergence to equilibrium for iterated function systems. *J. Phys. A* **2016**, *49*, 274001.
17. Lasota, A.; Mackey, M. *Chaos, Fractals, and Noise. Stochastic Aspects of Dynamics*, 2nd ed.; Springer-Verlag: New York, NY, USA, 1994.
18. Viana, M. *Lectures on Lyapunov Exponents*; Cambridge University Press: Cambridge, UK, 2014.
19. Baladi, V. Decay of correlations. In *Proceedings of Symposia in Pure Mathematics*; American Mathematical Society: Providence, RI, USA, 2001; Volume 69.
20. Tsuda, I. Dynamic link of memory—Chaotic memory map in nonequilibrium neural networks. *Neural Netw.* **1992**, *5*, 313–326.
21. Tsuda, I. (Chubu University). Personal communication, 2016.
22. Galatolo, S.; Nisoli, I.; Saussol, B. An elementary way to rigorously estimate convergence to equilibrium and escape rates. *J. Comput. Dyn.* **2015**, *2*, 51–64.



© 2018 by the authors. Licensee MDPI, Basel, Switzerland. This article is an open access article distributed under the terms and conditions of the Creative Commons Attribution (CC BY) license (<http://creativecommons.org/licenses/by/4.0/>).